

A High-Resolution Transmission Electron Microscopy Study of MBE Grown GaAs/Al_{0.3}Ga_{0.7}As Layers

(MBE로 성장시킨 GaAs/Al_{0.3}Ga_{0.7}As 층의 고분해능
투과전자현미경에 의한 연구)

李 廷 鎔*

(Jeong Yong Lee)

要 約

MBE로 성장시킨 GaAs/Al_{0.3}Ga_{0.7}As층에서 well과 barrier 및 계면의 원자 배열을 원자규모로 파악하기 위하여 단면시편을 만들어 고분해능의 투과전자현미경을 사용하여 연구하였다.

실험결과, 전자현미경 상에서 GaAs와 Al_{0.3}Ga_{0.7}As 및 모든 계면의 원자구조를 직접 알 수 있었다. Well과 barrier의 두께도 원자규모로 측정 가능하다. GaAs와 Al_{0.3}Ga_{0.7}As계면은 구분이 명확하나 원자규모로 볼 때 평탄하지 않고, 수개의 {002} GaAs 면간격 높이에 해당하는 언덕이 존재하기 때문에 계면이 평탄하지 않게 된다. 계면에서의 원자배열은 구조적인 무질서가 전혀없이 거의 완벽하게 정합이 되어 있다. 계면에서 합금 원소의 집합현상은 관찰되지 않았다.

Abstract

A cross-sectional transmission electron microscopy study of the MBE grown GaAs/Al_{0.3}Ga_{0.7}As layers was carried out at high-resolution so that the atomic arrangement of the well, barrier and the interface could be understood on an atomic level.

Results show that the images reveal directly the atomic structure of the GaAs, Al_{0.3}Ga_{0.7}As layers, and all internal interfaces. The well and barrier thicknesses can be measured on the atomic scale. The GaAs/Al_{0.3}Ga_{0.7}As interface is sharply defined but is not smooth on the atomic scale. The roughness arises from the presence of hills with heights of several {002} GaAs interplanar spacings. The atomic arrangement at the interface is almost completely coherent without any structural disorder. Alloy clustering at the interface was not observed.

*正會員, 韓國科學技術大學 電子材料科
(Dept. of Materials Science and Eng., Korea
Institute of Technology)
接受日字: 1989年 4月 12日

I. Introduction

The superlattices, or quantum well structures, which consist of alternating layers of two semiconductors, have attracted considerable attention for

application to quantum well lasers, very high performance field effect transistors (FETs), two dimensional electron gas field effect transistors (2DEG-FETs), high electron mobility transistors (HEMTs), and modulation doped field effect transistors (MODFETs). GaAs/(Al,Ga)As semiconductor heterostructures are the most widely studied, since the two materials have the same crystal structure and they have almost equal lattice constants and thus the structures tend to form with a minimum amount of defecting at the interface.

Energy levels in GaAs/(Al,Ga)As heterostructures are functions of the well thickness (L_a) and barrier thickness (L_b). In GaAs/(Al, Ga)As quantum wells, the photoluminescence (PL) peak energy, that is, the transition energy between electronic states in the confined well, is dependent on the well thickness and optical transitions involving unconfined states are dependent on the barrier thickness. The photoluminescence spectrum changes systematically with the barrier thickness. The formation of so-called islands in the hetero-interface results in fluctuation in well thickness and thus changes the line width of the photoluminescence spectrum and that of the luminescence spectrum.^[1] The photoluminescence spectral width is completely related to the interface roughness which is dependent on the growth method and growth condition.^[2] Since crystal quality in actual devices improves with growth temperature, the capability of growing abrupt interfaces at higher temperatures is important. However, the interface becomes rough as the growth temperature increases in molecular beam epitaxy (MBE) technology, where it is almost impossible to grow the superlattices at temperatures higher than 650°C. Thus, it is essential to measure the well and barrier thicknesses accurately and to study the atomic arrangement of the interface in order to get informations to obtain the better performance of devices.

There are several techniques to measure these important structural parameters. Photoluminescence excitation (PLE) measurements yield accurate sample parameters when they can be determined by theoretical fittings. However, this technique requires time-consuming curve fitting processes. Raman spectroscopy of phonons provides the most accurate value for the aluminum composition, but does not yield informations on

the well thickness and barrier thickness easily. X-ray double crystal diffractometry is a very useful technique since the well thickness and the alloy composition can be determined from one measurement.^[3] However, the determined values are not usually as accurate compared to those derived by other techniques. Cross-sectional transmission electron microscopy (TEM) provides the well and barrier thicknesses of the samples directly on the atomic scale. One of the most important factor in the GaAs/(Al, Ga)As heterostructure is the regular lattice arrangement across the interface. Furthermore, the direct method of studying the abruptness of heterointerfaces is the observation of the lattice arrangement at the interfaces by cross-sectional high-resolution transmission electron images. Cross-section transmission electron microscopy specimens were found to be extremely difficult to prepare. However, the potential wealth of information available justified the effort.

II. Experimental Procedure

The samples consisted of five alternating layers with total thickness of about 1000 nm: (1) Al_{0.3}Ga_{0.7}As barrier, (2) GaAs well, (3) Al_{0.3}Ga_{0.7}As barrier, (4) GaAs well, and (5) Al_{0.3}Ga_{0.7}As barrier. These layers were grown on a GaAs substrate with a (001) growth surface by molecular beam epitaxy at 580°C. AlAs mole fraction (x) of 0.3 was chosen for Al _{x} Ga_{1- x} As layer because with that value of x , the highest quasi-two-dimensional electron gas mobility was obtained.^[4] The barrier are sufficiently thick so that the tunneling effects are insignificant for this study.

Two samples were bonded face to face with epoxy and then squeezed with a clip to minimize the epoxy layer thickness between two samples. After a minimum setting period of 1 day, the bonded samples were mounted with wax (80°C melting point) onto a quartz disc so that the interesting interfaces were perpendicular to the plane of the disc. The sample was polished mechanically on a rotating wheel with 600 grit paper. The final polishing was accomplished with 0.03 μ m alumina paste. This polishing procedure was repeated on the other side of the specimen until a final thickness of between 50 and 100 μ m was achieved. The sample was separated from the

quartz disc by dissolving the wax in a beaker of ethanol. The sample was then dried and glued to a copper grid for support and easy handling.

The rotating specimen stage of the Gatan ion mill, cooled with liquid nitrogen, was used for ion beam milling at 17° gun tilt, 5 kV gun voltage and $50 \mu\text{A}$ specimen current. The final milling was accomplished with at 12° gun tilt, $10 \mu\text{A}$ specimen current. A higher yield of good specimens can be obtained if more mechanically thinning is employed, because this reduces the preferential ion beam milling effect on the epoxy. High-resolution micrographs were obtained by a JEOL JEM 200CX electron microscope with a high-resolution pole piece, operated at 200 keV.

III. Results and Discussion

Figure 1 shows a bright field transmission electron microscopy image of the sample obtained by cross-sectional TEM specimen preparation as described above. In this figure, there are five layers between the GaAs substrate at the bottom and the amorphous epoxy layer on the top surface which was included for the specimen preparation. The first layer on the GaAs substrate was identified as $\text{Al}_{0.3}\text{Ga}_{0.7}\text{As}$ layer since this layer showed the lighter contrast compared to the GaAs substrate. The higher scattering factor of Ga atoms in the GaAs layer as compared to Al atoms in the $\text{Al}_{0.3}\text{Ga}_{0.7}\text{As}$ layer leads to the darker contrast for the GaAs layer in the bright field TEM image where the objective aperture removes electron beams coming from high angles through the optic axis. Using the magnification standard at the bottom on the electron micrograph negative film of this figure, the well and barrier thicknesses were measured. It was found that the first barrier layer is 230 nm thick. The magnification standard was calibrated using diffraction grating replicas for accurate magnification measurements from electron micrographs. The second and fourth layers from the substrate with the darker contrast compared to $\text{Al}_{0.3}\text{Ga}_{0.7}\text{As}$ are 197 nm thick and 216 nm thick GaAs wells, respectively, whereas the third and fifth layers with the lighter contrast are both 210 nm thick $\text{Al}_{0.3}\text{Ga}_{0.7}\text{As}$ barriers. These values are in close agreement with those estimated from the growth rates. Both the GaAs and $\text{Al}_{0.3}\text{Ga}_{0.7}\text{As}$ layers are highly uniform and it seems that there is no structural disorder at the interface in this figure.

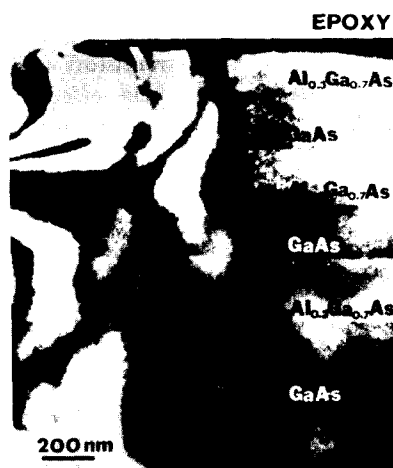


Fig. 1. Bright-field TEM image of the GaAs/ $\text{Al}_{0.3}\text{Ga}_{0.7}\text{As}$ layers on the GaAs substrate.

Figure 2 shows the completely-indexed $[1\bar{1}0]$ GaAs $\parallel [1\bar{1}0]$ $\text{Al}_{0.3}\text{Ga}_{0.7}\text{As}$ selected area diffraction (SAD) pattern which was obtained by the area in Fig. 1. Since it is impossible to discern between the GaAs spots and $\text{Al}_{0.3}\text{Ga}_{0.7}\text{As}$ spots in this diffraction pattern, it is clear that all the GaAs reflections are completely coincident with $\text{Al}_{0.3}\text{Ga}_{0.7}\text{As}$ reflections with a parallel orientation relationship. This fact indicates that the lattice constants of GaAs and $\text{Al}_{0.3}\text{Ga}_{0.7}\text{As}$ are nearly the same and there is a negligible misfit between GaAs and $\text{Al}_{0.3}\text{Ga}_{0.7}\text{As}$ lattice parameters. In fact, the lattice constant of GaAs ($a=0.56523 \text{ nm}$)^[5] is very similar to that of AlAs ($a=0.56605 \text{ nm}$) with a 0.13 % misfit,^[3] which implies that there is a negligible lattice misfit between GaAs and $\text{Al}_{0.3}\text{Ga}_{0.7}\text{As}$, and that the atomic arrangement at the GaAs/ $\text{Al}_{0.3}\text{Ga}_{0.7}\text{As}$ interface is very regular without misfit dislocations.

Analysis of these diffraction patterns shows that both GaAs and $\text{Al}_{0.3}\text{Ga}_{0.7}\text{As}$ have a face-centered cubic (fcc) lattice with the lattice parameter 0.565 nm. GaAs and $\text{Al}_{0.3}\text{Ga}_{0.7}\text{As}$ have the zincblende structure. GaAs structure has an fcc lattice with a basis of one GaAs molecule, one atom at 000, and the other at $\frac{1}{4}\frac{1}{4}\frac{1}{4}$ of the non-primitive face-centered cubic unit cube, whereas

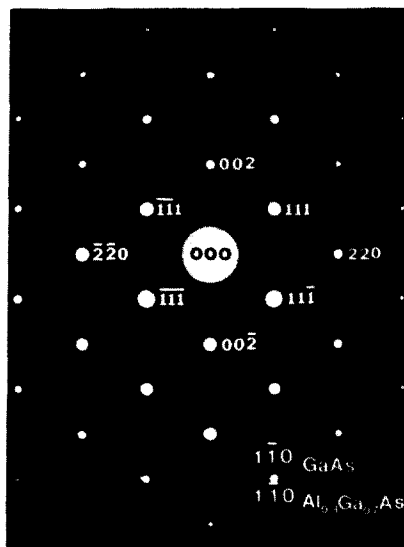


Fig.2. Selected area diffraction pattern in a $\langle 110 \rangle$ GaAs and Al_{0.3}Ga_{0.7}As zone axis orientation. Superimposed $[1\bar{1}0]_{\text{GaAs}}$ and $[1\bar{1}0]_{\text{Al}_{0.3}\text{Ga}_{0.7}\text{As}}$ zone axes are shown on the SAD pattern in the bottom-right corner. Note that the reflections from two crystals are completely coincident with a parallel orientation relationship.

AlAs structure has an fcc lattice with a basis of one AlAs molecule, one Al atom at 000, and one As atom at $\frac{1}{4}\frac{1}{4}\frac{1}{4}$. Al_{0.3}Ga_{0.7}As is a solid solution of GaAs and AlAs with the AlAs mole fraction 0.3. In this orientation, the eight spots immediately surrounding the forward-scattered beam are the first-order $[1\bar{1}0]$ reflections. The $\{111\}$ and $\{002\}$ reflections represent lattice spacings of about 0.323nm and 0.28nm, respectively. In this electron diffraction pattern, there is no satellite spot around the main diffraction spots, since the spacing of the layers is very wide compared to that of GaAs $\{002\}$ planes, and the superlattice reflection is supposed to be nearly coincident with the main diffraction spot. In addition, there is no streak from the reflections, implying that there is no sufficient density of thin planar defects (twins, stacking faults or second phases) which is enough to contribute to the electron diffraction.

In the diffraction pattern, the intensity of $\{002\}$ reflections is not so weak compared to

those of other first-order reflections. However, calculated intensity of the (002) reflection for GaAs, $16(f_{\text{Ga}} - f_{\text{As}})^2$, is nearly zero,^[6] and the intensity for Al_{0.3}Ga_{0.7}As, $16(0.3f_{\text{Al}} + 0.7f_{\text{Ga}} - f_{\text{As}})^2$, has a lower value compared to the intensities of other reflections, $16(f_{\text{Ga}} + f_{\text{As}})^2$, or $16(0.3f_{\text{Al}} + 0.7f_{\text{Ga}} + f_{\text{As}})^2$, where f_{Ga} , f_{As} and f_{Al} are the atomic scattering factors of Ga, As and Al, respectively. The relatively strong intensity of $\{002\}$ reflections in this figure, which was supposed to be weak from the kinematical intensity calculation, can arise due to double diffraction. For example, diffracted intensity can occur in the (002) position by double diffraction from the (111) and $(\bar{1}\bar{1}1)$ reflection spots from GaAs or Al_{0.3}Ga_{0.7}As, i.e. $(111) + (\bar{1}\bar{1}1) = (002)$. It is possible to determine whether or not certain forbidden reflections are present due to double diffraction by tilting the crystal about the axis containing the forbidden reflections. If the forbidden spots disappear after the crystal has been tilted to the extent that intensity from the reflection outside of the forbidden row can no longer contribute toward double diffraction, then it may be concluded that the spots are due to double diffraction. This tilting experiment was applied to determine whether or not the $\{002\}$, $h+k+l=4n+2$ reflections are due to double diffraction. The result shows that the $\{200\}$ spots do not persist so strong as the crystal is tilted to obtain a $\langle 100 \rangle$ zone axis orientation. The $\{200\}$, $\{420\}$ reflections in $[100]$ zone axis diffraction pattern cannot occur by double diffraction. Thus it is concluded that these spots are due to double diffraction.

Figure 3 shows a low magnification high-resolution transmission electron microscopy image of the second GaAs/Al_{0.3}Ga_{0.7}As interface from the top in the area of Fig. 1. This axial lattice image was taken in a $\langle 110 \rangle$ zone axis orientation with an objective aperture, which contained only the forward-scattered beam and the eight spots immediately surrounding this beam, in order to enhance the contrast of two layers, since a smaller objective aperture can remove more scattered electrons with high angles. In this figure, the lower region with the darker contrast are GaAs whereas the upper region is Al_{0.3}Ga_{0.7}As with the lighter contrast. Since the atomic scattering factors of Ga and Al atoms are almost identical, it is expected that the contrast of the two layers

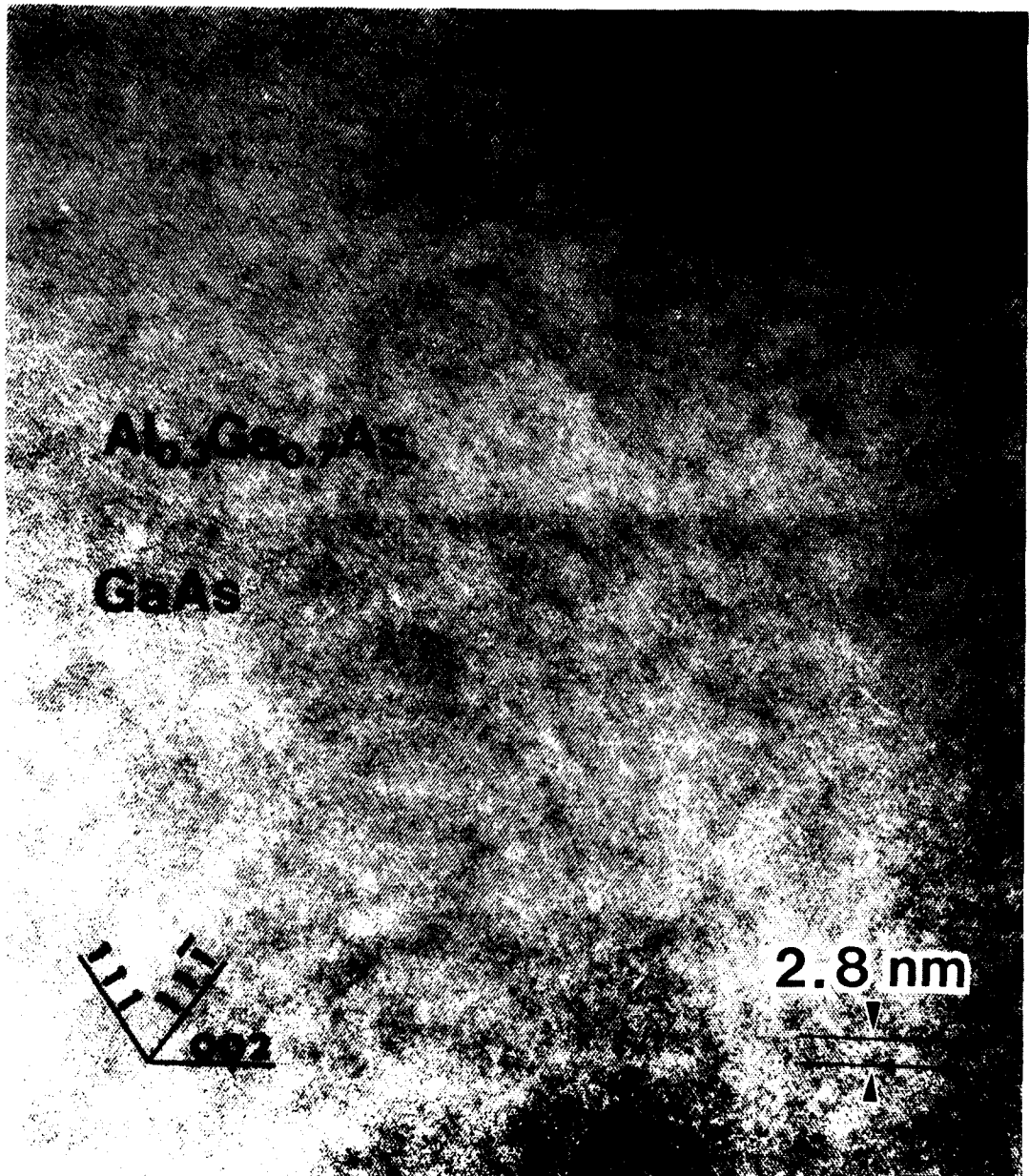


Fig.3. Low magnification high-resolution TEM image of the GaAs/Al_{0.3}Ga_{0.7} layers in a <110> orientation.

is verly low.[7] However, this image clearly reveals the atomic structure of the GaAs, Al_{0.3}Ga_{0.7}As layers, and the interface.

Two major crystallographic planes, {111} and {002}, are superimposed on the GaAs lattice

image in the bottom-left corner, and ten {002} spacings of GaAs are indicated by the marker in the bottom-right corner of this figure. Comparing these planes with the macroscopic GaAs/Al_{0.3}Ga_{0.7}As interface shows that the interface is a

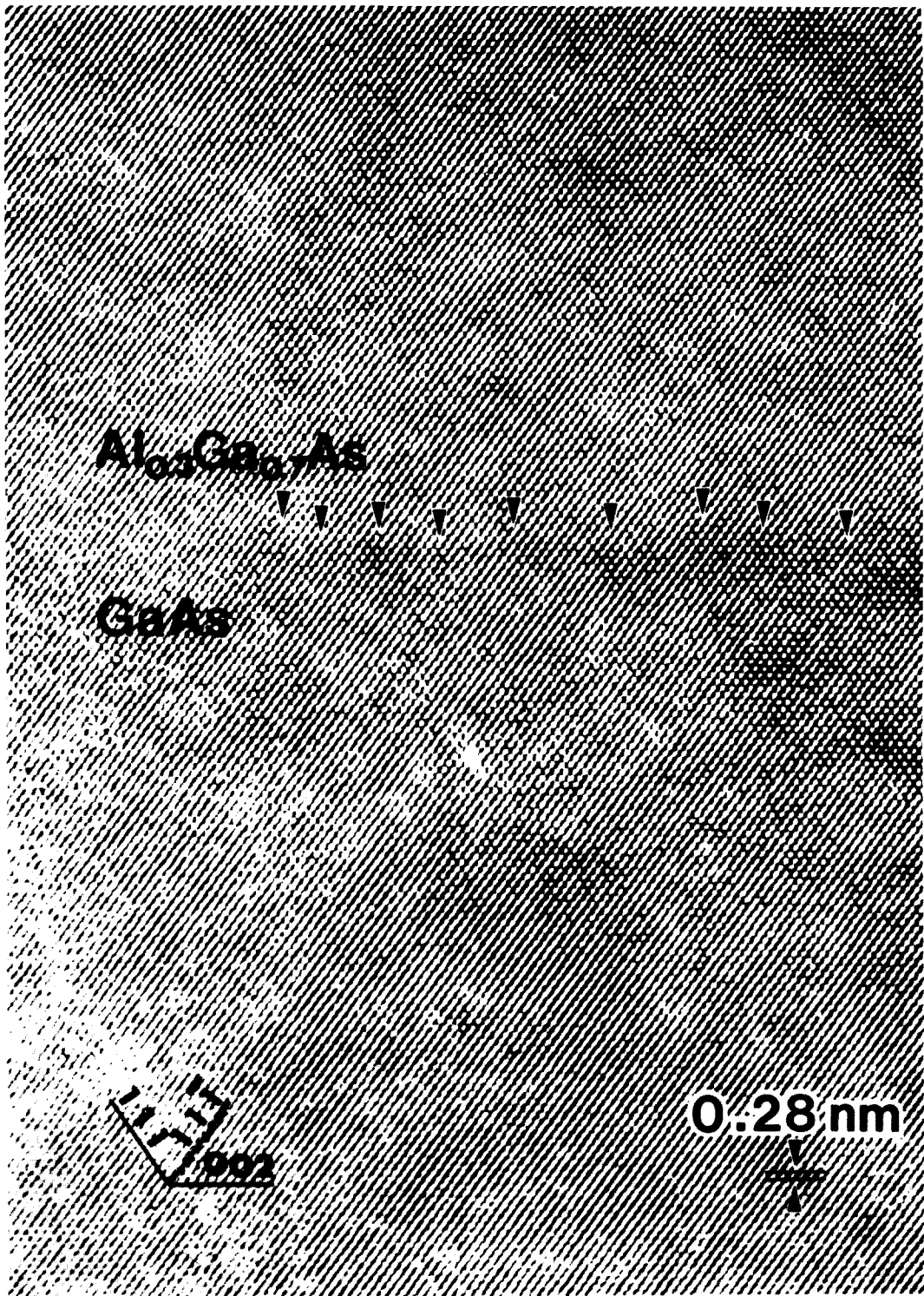


Fig.4. High-resolution TEM image of the GaAs/ $\text{Al}_{0.3}\text{Ga}_{0.7}\text{As}$ interface showing the roughness of the atomic arrangement at the interface.

{002} plane of the GaAs and $\text{Al}_{0.3}\text{Ga}_{0.7}\text{As}$ layers, implying that the growth direction of the GaAs and $\text{Al}_{0.3}\text{Ga}_{0.7}\text{As}$ layers is a $\langle 001 \rangle$ direction. It is easily seen that the interface is sharply defined and seems to be smooth. Using the 0.28 nm spacing of the {002} GaAs planes as an internal magnification standard, it was found that the GaAs well layer is 196.8 nm thick, which corresponds to heights of 703 {002} GaAs spacings on the electron micrograph negative. Thus, the well and barrier thicknesses can be accurately measured on the atomic scale. By sighting along the (111) GaAs planes, it is clear that all the GaAs (111) planes are continuous as they cross the GaAs/ $\text{Al}_{0.3}\text{Ga}_{0.7}\text{As}$ interface. By sighting along other GaAs planes, it also shows that these planes are continuous across the interface. Furthermore, it is clearly seen that there is no noticeable contrast change in the GaAs and $\text{Al}_{0.3}\text{Ga}_{0.7}\text{As}$ layers, that is, a uniform contrast for each layer, even though there is a thickness change of the specimen. Thus, it is concluded that there is no structural irregularity such as dislocations, stacking faults or twins.

Figure 4 shows an enlargement of the high-resolution transmission electron microscopy image of the GaAs/ $\text{Al}_{0.3}\text{Ga}_{0.7}\text{As}$ interface of Fig. 3, again taken in a $\langle 110 \rangle$ zone axis orientation. The interface character is shown in greater detail in this enlargement of the interface. The crystallographic planes, {111} and {002}, and the {002} spacing in the GaAs region are indicated in the bottom-left and bottom-right corners of this figure, respectively.

By sighting along the (111) GaAs planes, it is concluded that these planes are continuous as they cross the interface and become the (111) $\text{Al}_{0.3}\text{Ga}_{0.7}\text{As}$ planes and that the interface is almost completely coherent. Again, sighting along other planes shows that these planes are also continuous as they cross the interface and the interface is largely coherent with a parallel orientation relationship, which is also indicated by the selected area diffraction pattern in Fig. 2. Comparing these planes with the GaAs/ $\text{Al}_{0.3}\text{Ga}_{0.7}\text{As}$ interface shows that the macroscopic interfacial plane is close to a {002} plane of the GaAs and $\text{Al}_{0.3}\text{Ga}_{0.7}\text{As}$ crystals. It is easily seen that interface is sharply defined but is not smooth on the atomic scale. By sighting carefully along the {002} interfacial plane, it is possible to find that the lower GaAs region with the darker contrast

protrudes into the upper $\text{Al}_{0.3}\text{Ga}_{0.7}\text{As}$ region with the lighter contrast as indicated by arrowheads in the figure. The roughness arises from the presence of hills with heights of several {002} GaAs interplanar spacings as indicated by the superimposed arrowheads. These hills or valleys lead to the fluctuation in well thickness.

The interface roughness is dependent on the growth condition. It has generally been accepted that the interface becomes rough as the growth temperature increases in MBE technology, where it is almost impossible to grow the superlattices at temperatures higher than 650°C. However, in metalorganic chemical vapor deposition (MOCVD), the apparent interface roughness evaluated from the photoluminescence spectra improves as the growth temperature increases and no jamming of superlattice has been experienced to above 800°C,^[2] since the growth mechanism in the surface reaction is different for the two technologies. Watanabe and Mori^[2] explained the narrower peaks of the spectra from the quantum wells grown at higher temperature on a model where the size of the hills and/or valleys on the interface grown by MOCVD at higher temperature is smaller. Kajiwara et al.^[1] observed the fluctuation in thickness of the GaAs and AlAs layers which resulted in formation of so-called islands. In the samples grown by MOCVD, the variation of the PL line width indicated the fluctuation in well thickness with one atomic layer.^[8] Thus, it is expected that, in the present sample which was grown by MBE at 580°C, the interface roughness due to the presence of hills with the heights of several atomic layers will also lead to a change in the PL spectrum width.

No irregularity in the contrast of the image in Fig. 4 is observed in the $\text{Al}_{0.3}\text{Ga}_{0.7}\text{As}$ layer, which indicates that the alloy clustering^[9] in the $\text{Al}_{0.3}\text{Ga}_{0.7}\text{As}$ barriers, where the aluminum concentration is nearly zero, does not occur in the present sample.

IV. Conclusions

A cross-sectional transmission electron microscopy study of the MBE grown GaAs/ $\text{Al}_{0.3}\text{Ga}_{0.7}\text{As}$ layers was carried out at high-resolution so that the atomic arrangement of the well, barrier and the interface could be understood on an

atomic level. The images reveal directly the atomic structure of the GaAs, Al_{0.3}Ga_{0.7}As layers, and all internal interfaces. The following results have been obtained:

1. The well and barrier thicknesses can be measured on the atomic scale.
2. The GaAs/Al_{0.3}Ga_{0.7}As interface is sharply defined but is not smooth on the atomic scale. The roughness arises from the presence of hills with heights of several {002} GaAs interplanar spacings.
3. The atomic arrangement at the interface is almost completely coherent without any structural disorder.
4. Alloy clustering was not observed.

References

- [1] K. Kajiwara, H. Kawai, K. Kaneko and N. Watanabe, "Structure of MOCVD grown AlAs/GaAs hetero-interfaces observed by transmission electron microscopy," *Jap. J. Appl. Phys.*, 24, pp. L85-L88, 1985.
- [2] N. Watanabe and Y. Mori, "Ultrathin GaAs/GaAlAs layers grown by MOCVD and their structural characterization," *Surf. Sci.*, 174, pp. 10-18, 1986.
- [3] T. Ishibashi, Y. Suzuki and H. Okamoto, "Photoluminescence of an AlAs/GaAs superlattice grown by MBE in the 0.7-0.8 μm wavelength region," *Jap. J. Appl. Phys.*, 20, pp. L623-L626, 1981.
- [4] S. Hiyamizu, J. Saito, K. Nanbu and T. Ishigawa, "Improved electron mobility higher than 10^{10} cm²/Vs in selectively doped GaAs/N-AlGaAs heterostructures grown by MBE," *Jap. J. Appl. Phys.*, 22, pp. L609-L611, 1983.
- [5] J.S. Blakemore, "Semiconducting and other major properties of gallium arsenide," *J. Appl. Phys.*, 53, pp. R123-R181, 1982.
- [6] H. Okamoto, M. Seki and Y. Horikoshi, "Direct observation of lattice arrangement in MBE grown GaAs-AlGaAs superlattice," *Jap. J. Appl. Phys.*, 22, pp. L367-L369, 1983.
- [7] Y. Suzuki and H. Okamoto, "High contrast TEM observation of lattice image of GaAs-AlGaAs superlattice with [100] electron beam incidence," *Surf. Sci.*, 174, pp. 82-83, 1986.
- [8] H. Kawai, J. Kaneko and N. Watanabe, "Doublet state of resonantly coupled AlGaAs/GaAs quantum wells grown by metalorganic chemical vapor deposition," *J. Appl. Phys.*, 58, pp. 1263-1269, 1983.
- [9] N. Holonyak, Jr., W.D. Laidig and B.A. Vojak, "Alloy clustering in Al_xGa_{1-x}As-GaAs quantum-well heterostructures," *Phys. Rev. Lett.*, 45, pp. 1703-1706, 1980. *

著者紹介



李廷鎔(正會員)

1951年 12月 12日生. 1974年 2月 서울대학교 재료공학과 졸업 학사 학위 취득. 1976년 2월 한국과학기술원 재료공학과 졸업 석사학위 취득. 1976년~1981년 금성사/ 금성정밀 중앙연구소 재직. 1981년~1986년 미국 Univ. of California, Berkeley 재료공학과 박사학위 취득. 1981년~1986년 미국 Lawrence Berkeley Laboratory 재직. 1986년 7월~현재 한국과학기술대학 전자재료과 조교수. 주관심분야는 전자현미경학임.